ISSN 1070-4272, Russian Journal of Applied Chemistry, 2023, Vol. 96, No. 12, pp. 1063–1075. © Pleiades Publishing, Ltd., 2023.
Russian Text © The Author(s), 2023, published in Zhurnal Prikladnoi Khimii, 2023, Vol. 96, No. 12, pp. 980–993.

APPLIED ELECTROCHEMISTRY
AND METAL CORROSION PROTECTION

Electrochemical Deposition of Iridium onto Gallium Arsenide from a Sulfamate Electrolyte Based on Hexachloroiridic(IV) Acid

T. P. Bekezina[a],*, M. S. Vaisbekker[a],, V. A. Burmistrova[a], and V. G. Bozhkov[a]**

[a] *Research Institute of Semiconductor Devices, Tomsk, 634034 Russia*
**e-mail: t-bekezina@mail.ru*
***e-mail: mariya_vaisbekker@mail.ru*

Received December 20, 2023; revised December 28, 2023; accepted December 29, 2023

Abstract—The nature of cathodic polarization in an iridium-plating electrolyte based on a sulfamate solution of $H_2[IrCl_6]$ was studied. Spectroscopic analysis shows that the iridium electrolyte contains binuclear oxygen-bridged Ir(III, IV) sulfamate complexes. The microstructure and distribution profiles of the iridium deposit in contacts of different diameters were studied. The structure of the iridium deposit is highly dispersed. The nonuniformity of the iridium deposit profile over the contact area and the dependence of the deposit thickness on the contact diameter can be reduced by varying the hydrodynamic conditions of the metal electroplating (stirring of the electrolyte with a magnetic stirrer or ultrasound) and by using electrochemical polarization. The Ir–GaAs contacts with the Schottky barrier are characterized by high quality of electrophysical parameters and good reproducibility of the volt–ampere characteristics. A decrease in the thickness of the iridium deposit and of the n-GaAs epitaxial layer leads to an increase in the barrier height of the rectifying Ir–GaAs contacts.

Keywords: iridium, electrochemical deposition, gallium arsenide, activation energy, UV–visible spectroscopy, IR spectroscopy, atomic-force microscopy, Schottky barriers, sulfamate electrolytes, hexachloroiridic acid

DOI: 10.1134/S1070427223120066

Iridium can be used in semiconductor microelectronics, in particular, for making diodes based on contacts with the Schottky barrier. This metal is high-melting (melting point ~2447 K), highly inert chemically, and resistant to oxidation [1]. Ir–GaAs contacts with the Schottky barrier, prepared by electron-beam sputtering, have uniform and finely grained structure and preserve good parameters upon short annealing (for 10 s) at temperatures of at least up to 800°C [2]. Among the platinum group metals studied, iridium has the maximal activation energy of the interaction in the M–GaAs system (~3.15 eV). The interfacial interaction of iridium with gallium arsenide occurs in the interval 500–650°C (onset at 500°C) [2–4]. In semiconductor devices, iridium is mainly used for preparing contacts with the Schottky barrier to gallium nitride (GaN) and to various heterostructures based on it [5–8] and as diffusion barriers [9]. Thin iridium films for these purposes are mainly prepared by magnetron and electron-beam sputtering. These two processes require sophisticated and expensive equipment. In addition, iridium has a very high melting point, which complicates the metal deposition onto a semiconductor by physical methods. In many cases, this problem is solved by the metal electroplating.

Chloride, bromide, bromate, sulfate, sulfamate, phosphate, and alkaline electrolytes are used for the electrodeposition of iridium coatings onto metals [10]. The most cost-saving and stable electrolytes are sulfamate electrolytes based on iridium chloride compounds [11] and electrolytes prepared by dissolving iridium metal in sulfamic acid under the action of alternating current (AC) of industrial frequency [12].

The first attempts to prepare electroplated contacts of Ir to GaAs were made by Batenkov et al.; they used electrolytes prepared by dissolving iridium metal in hydrochloric and sulfamic acid solutions under the action of AC [13–15]. However, the procedure for preparing electrolytes used by Batenkov et al. is labor-consuming,

and the electrolytes undergo rapid aging. The iridium electrodeposition from the sulfamate electrolyte occurs at elevated temperatures with low current efficiency (~0.5–0.6%), and the electrophysical characteristics of the contacts are relatively poor. In addition, the iridium contacts prepared by these procedure exhibit low resistance to elevated temperatures and prolonged keeping in air.

The development of an electrolyte for the electrochemical deposition of Ir onto GaAs was a significant step to preparation of high-quality Ir–GaAs contacts with the Schottky barrier [16]. The electrolyte contained iridium sulfamate complexes of unidentified structure, formed in an aqueous solution containing (g L^{-1}) hexachloroiridic acid ($H_2[IrCl_6]$) (3–6.5 in terms of Ir) and sulfamic acid (H_3NSO_3) (30–60) upon heating of the solution on a water bath at approximately 100°C for 3–4 h until the initially red-brown solution acquired a stable orange-yellow (salmon) color. In [17], we studied in detail the electrophysical parameters of Ir–GaAs contacts with the Schottky barrier, prepared from this electrolyte. The thermal stability of Ir–GaAs contacts and of contacts with two-layer metal plating, Pt/Ir–GaAs, under the conditions of short heat treatment (for 10 min in a hydrogen atmosphere) in the interval 300–550°C was considered in [18]. The iridium plating electrolyte used in that study allows preparation of high-quality heat-resistant (up to 550°C) rectifying contacts Ir–GaAs and Pt/Ir–GaAs with the electrophysical characteristics close to the ideal values. A specific feature of the results is higher heat resistance of contacts with small diameters.

This study was aimed at elucidating the nature of the cathodic polarization in the electrodeposition of Ir onto *n*-GaAs from the iridium plating electrolyte developed, at determining the composition of the iridium complexes, the morphology of the contact surface, and the distribution profiles of Ir deposits in windows of different diameters, and at preparing Ir–GaAs rectifying contacts with high and well reproducible electrophysical characteristics.

EXPERIMENTAL

Experiments were performed with commercial structures n–n^+-GaAs (100) (SAG-4, SAG-4B, Elma-Malakhit, Russia) doped with tin and grown by the OMC–hydride procedure [gas-phase epitaxy from a gallium organometallic compound, $Ga(CH_3)_3$, and arsine, AsH_3] [19], with the epitaxial layer thickness (l) of 0.7–1.0 μm and heterogeneous distribution of the dopant (N_D): concentration of 8 × 10^{16} cm^{-3} in the surface 0.2-μm layer and 3 × 10^{16} cm^{-3} in the other parts. In some cases, we used structures obtained also by OMC–hydride epitaxy (Research Institute of Semiconductor Devices, Russia) with the *n*-layer thickness of 0.3 μm and dopant concentration of 6 × 10^{16} cm^{-3}. The ohmic contact from the n^+-layer side (N_D = 2 × 10^{18} cm^{-3}) was made by the electrodeposition of the AuGe alloy (0.2 μm), followed by annealing in a hydrogen atmosphere at 400°C for 10 min and subsequent deposition of a 2-μm-thick gold layer [20].

The cathodic polarization curves were recorded in the potentiodynamic mode with an IPC-Pro M potentiostat–galvanostat (Volta, Russia). The polarization measurements were performed in a three-electrode quartz electrochemical cell. GaAs samples with the working surface area of 0.1–0.2 cm^2 were used as cathodes. Prior to polarization measurements, the sample surface was chemically treated in an ammonia–peroxide etching solution of the composition NH_4OH : H_2O_2 : H_2O = 10 : 3.5 : 500 (ultrapure grade chemicals produced by Sigma-Tech were used) for 10 s with the calculated etching rate of 0.12 μm min^{-1}, washed with deionized water of grade A, OST (Branch Standard) 11.029.003-80 (Research Institute of Semiconductor Devices), resistance 18 MΩ, for 30 s, and treated with an ammonia solution of the composition NH_4OH : H_2O = 1 : 5 in an ultrasonic field for 20 s. After that, the samples were again washed with water for 30 s and dried in a flow of gaseous nitrogen of grade 5.0 (Horst, Russia). According to the data of contact voltammetry and X-ray photoelectron spectroscopy [21], treatment of gallium arsenide in a polishing ammonia etching solution leads to the formation of the surface oxide $GaAsO_4$ in which both components of GaAs are in the highest oxidation states. The phases of elemental arsenic and oxide As_2O_3, responsible for the formation of surface electronic states [22], are virtually absent. The subsequent treatment (decapping) in an ammonia solution favors the dissolution of $GaAsO_4$. The finishing treatment in deionized water leads to the predominant formation of Ga_2O_3 on the gallium arsenide surface. The ohmic contacts and nonworking surface of the samples were protected with KhV-784 chemically durable lacquer (YarLI Research and Production Company, Russia). A platinum plate of Pl99.9 grade (ENTsM, Russia) served

as a counter electrode, and a platinum wire of grade Pl99.9 (ENTsM) mounted in a Teflon holder served as a reference electrode. The potential of the platinum wire electrode was measured vs. saturated silver chloride electrode (SSCE) in a separate electrolyte sector. All the potentials are given vs. SSCE.

The electrolytes were prepared using aqueous $H_2[IrCl_6]$ with the iridium content of 19.94 and 20.71% (pure and analytically pure grades, respectively; Aurat, Russia), H_3NSO_3 of chemically pure grade (VEKTON, Russia), and deionized water. The experiments involving ultrasonic treatment were performed with a temperature-controlled ultrasonic bath of PSB-1335-05 type (PSB-GALS, Russia). The constant temperature in the cell was maintained using this ultrasonic bath. The accurate temperature of the electrolyte in the cell was measured with a mercury thermometer.

To elucidate the nature of the cathodic polarization in the iridium electrodeposition, we used the temperature-kinetic method [23]. Experiments were performed in the electrolyte of the initial composition (g L^{-1}) 5 $H_2[IrCl_6]$ (in terms of iridium) and 50 H_3NSO_3 in the temperature interval 20–65°C. Using a series of cathodic polarization curves recorded at different electrolyte temperatures, we plotted the dependences of the logarithm of the current density on the reciprocal temperature at potentials corresponding to the metal deposition range. The effective activation energy was calculated from the slope of the straight lines obtained.

The ionic composition of the iridium complexes in the electrolyte was studied by spectroscopic methods. The electronic absorption spectra in the UV–visible range were recorded with an Evolution 600 spectrometer (Thermo Scientific) in the wavelength range 200–900 nm. The spectrophotometric analysis was performed using quartz cells with the solution layer thickness of 0.1 cm. To record the spectra, the solutions were diluted as required. The IR spectra were recorded with a NICOLET 5700 FTIR Fourier IR spectrometer (Thermo Electron Corporation) with a built-in attenuated total reflection (ATR) attachment with a diamond crystal in the range 400–4000 cm^{-1}. Samples of solid phases were prepared by evaporation of the iridium electrolyte and drying in air.

Ir–GaAs contacts were prepared by the standard procedure involving a photolithographic process of iridium deposition via pattern in a SiO_2 dielectric film (template). The 0.5-μm-thick silicon oxide film was prepared by pyrolytic oxidation of monosilane (SiH_4 of grade 5.5, Horst, was used) at 360°C [24]. In the SiO_2 dielectric coating, using a photoresist template, we etched windows of different diameters in a solution of the composition HF : NH_4F : H_2O = 90 : 690 : 186 (vol %) (we used ultrapure grade chemicals, Sigma-Tec). The contact diameter (*D*) was varied from 5 to 500 μm. The iridium electrodeposition into the windows was performed in a two-electrode electrochemical cell in the galvanostatic mode with application of an ultrasonic field and without it. The thickness of the electroplated iridium layer was controlled by the deposition time and was varied from 50 to 250 nm. The coating thickness was measured with an MII-4M Linnik microinterferometer (EuroLab, Russia).

The initial treatment of the GaAs surface before applying the dielectric involved preliminary chemical cleaning (mainly for degreasing) by successive treatment in monoethanolamine (C_2H_7NO), dimethylformamide (C_3H_7NO), and isopropanol (i-C_3H_7OH) (we used ultrapure grade solvents, Reakhim, Russia). The finishing treatment of the gallium arsenide surface immediately before the iridium electrodeposition into the windows was performed similarly to the samples for the electrochemical studies.

The surface morphology of thin iridium coatings in contacts of different diameters was studied by atomic-force microscopy with a Solver-HV microscope (NT-MDT, Russia). The profiles of the metal deposit distribution in the windows and the deposit thickness were evaluated with an S-Neox confocal profilometer (Sensofar).

The volt–ampere characteristics of the contacts formed were measured with a Cascade Microtech M150 probe station using a B1500A analyzer of the electrical characteristics of semiconductor devices (Agilent Technologies). The main electrophysical parameters of the Ir–GaAs contacts with the Schottky barrier, namely, the effective (φ_{bi}, eV) and measured (φ_{bm}, eV) barrier height, ideality factor n, and series resistance R_s, were determined from the volt–ampere curves [18, 25].

RESULTS AND DISCUSSION

The cathodic potentiodynamic polarization curves recorded at different temperatures in the electrolyte studied can be divided into five sectors (Fig. 1). Two limiting current portions can be clearly seen in the curves

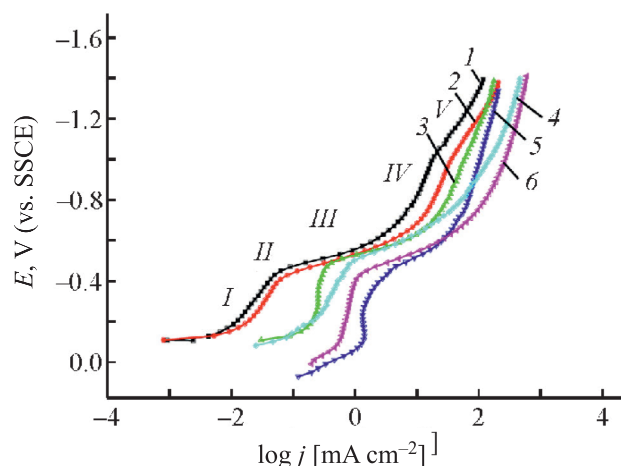

Fig. 1. Cathodic potentiodynamic polarization curves of n-type epitaxial gallium arsenide, recorded at different temperatures in a sulfamate iridium-plating electrolyte. Potential sweeping rate 20 mV s^{-1}; initial electrolyte composition (g L^{-1}): $H_2[IrCl_6]$ (in terms of iridium) 5 and H_3NSO_3 50. *T* (°C): (*1*) 23, (*2*) 35, (*3*) 45, (*4*) 45 with the applied ultrasonic field, (*5*) 65, and (*6*) 65 with the applied ultrasonic field.

(sectors *II*, *IV*). In a definite range of potentials, there is linear dependence between the potential and logarithm of the current density (sector *III*). The experiments have shown that, at current densities corresponding to the first two sectors, there is virtually no iridium deposition, and the current efficiency of the iridium deposition is close to zero. Presumably, in this range of current densities, complexes of tri- and tetravalent iridium are reduced to lower oxidation states. The electrolytic reduction of iridium to the metal, conjugated with the hydrogen evolution, occurs at current densities corresponding to the linear (Tafel) sectors of the polarization curve and the region of the second limiting current (sectors *III*, *IV*). After reaching the sector of the second limiting current, hydrogen evolution mainly occurs (sector *V*).

Table 1. Effective activation energy of iridium electrodeposition onto epitaxial structures $n–n^+$-GaAs (100) from sulfamate iridium-plating electrolyte

Electrode polarization *E*, V (SSCE)	Effective activation energy, kJ mol^{-1}
–0.45	83.7
–0.50	81.6
–0.55	58.9
–0.60	51.9
–0.65	46.5
–0.70	39.6
–0.80	36.3
–0.90	36.3
–1.00	34.5
–1.10	27.3

The polarization type was determined from the effective activation energy (Table 1). At potentials in the range from –0.45 to –0.60 V, corresponding to linear sectors of the polarization curves, the effective activation energy is in the range 84–52 kJ mol^{-1}, suggesting the electrochemical (kinetic) nature of the cathodic polarization. Thus, the slow step of the electrochemical reduction of iridium compounds to the metal in this range of potentials is the charge transfer through the interface. With an increase in the polarization, the activation energy gradually decreases from 52 to 27 kJ mol^{-1}. Hence, first the electrochemical polarization prevails (sector *III*); this interval is followed by the interval of mixed kinetics (sector *IV*) and then of the diffusion polarization (sector *V*).

Data on the iridium electrodeposition and the polarization measurements with the application of the ultrasonic field confirm the kinetic type of the polarization in the iridium-plating electrolytes at current densities corresponding to the Tafel sectors of the polarization curves. The linear sectors of the polarization curves recorded at 45 and 65°C with the application of the ultrasonic field (Fig. 1, curves *4*, *6*) and without it (Fig. 1, curves *3*, *5*) virtually coincide. The interval of the second limiting current due to diffusion restrictions is shifted toward higher current densities in the polarization curves recorded with the application of the ultrasonic field. The iridium electrodeposition rate only slightly increases on applying the ultrasonic field. However, according to the data of atomic-force microscopy, the iridium deposits have more finely grained structure in this case [16]. The iridium deposition rate at current densities corresponding to the potentials from –0.40 to –0.60 V is independent of stirring.

We have studied the effect of the current density, concentration of the initial electrolyte components, temperature, pH, and deposition conditions on the iridium deposition rate, current efficiency, and coating quality (adhesion, grain structure, continuity, metallic luster, etc.). The optimum composition of the starting components for preparing the iridium plating electrolyte was estimated theoretically and checked experimentally

at iridium concentrations in the interval 2.5–6.5 g L^{-1} and sulfamic acid concentrations in the interval 30–60 g L^{-1}. At the iridium concentration in the electrolyte decreased below 3 g L^{-1}, high-quality deposits could not be obtained at room temperature. The iridium coatings are dark and have no metallic luster. At the iridium concentration increased over 5 g L^{-1}, the deposit quality and current efficiency do not change noticeably. Therefore, it is not appropriate to take expensive iridium in a larger amount.

The pH of the iridium plating electrolyte is an important parameter. At pH of the electrolyte lower than 0.5, the current efficiency of the iridium deposition decreases because of the conjugate hydrogen evolution. At pH > 0, such reactions can occur in solution as aquation, hydration, and redox transformations [26], which can lead to a change in the electrolyte composition and to its rapid aging. The presence of sulfamic acid in the electrolyte is necessary not only for setting pH, but also for reducing the internal stresses in the deposit. Thus, the concentration of sulfamic acid required for the formation of complexes with iridium at iridium concentrations of 3–6.5 g L^{-1} with simultaneous maintenance of the required pH of the electrolyte is 30–60 g L^{-1}.

The influence of the current density on the iridium deposition rate and current efficiency was studied in the interval 0.05–3.5 A dm^{-2} (0.5–35 mA cm^{-2}) at the electrolyte temperatures of 20–80°C. As we found, at current densities lower than 0.1 A dm^{-2}, the iridium deposits are heterogeneous and have a honeycomb structure. In electrolysis at current densities higher than 3 A dm^{-2}, iridium black is formed. It is deposited in the form of small islets over the lustrous iridium deposit. In the electrodeposition from the electrolyte containing 5 g L^{-1} iridium at room temperature and a current density of 0.3–0.5 A dm^{-2}, the current efficiency of the iridium deposition is 9–14%, and the iridium deposition rate is 0.005–0.007 μm min^{-1}. At 60–65°C and a current density of 0.3 A dm^{-2}, high-quality iridium deposits were obtained with the current efficiency close to 100%, and the iridium deposition rate was 0.045 μm min^{-1}. The thickness of the iridium coating on gallium arsenide did not exceed 0.3 μm. The electrochemical deposition of iridium with the application of the ultrasonic field allows preparation of finely crystalline deposits.

The electrolyte is stable in operation and does not lose electrochemical activity after prolonged storage (for

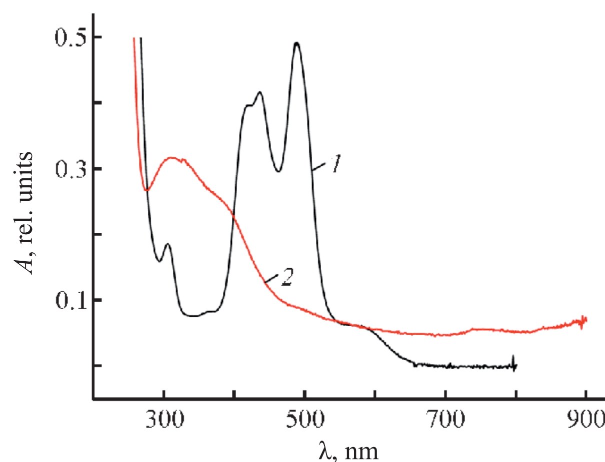

Fig. 2. Absorption spectra of sulfamate iridium-plating electrolytes. Initial electrolyte composition (g L^{-1}): $H_2[IrCl_6]$ (in terms of iridium) 5 and H_3NSO_3 50. (*1*) initial iridium-plating electrolyte (dilution 1 : 20) and (*2*) working iridium-plating electrolyte after 4-h heat treatment (dilution 1 : 10).

4 years) [16]. In repeated electrolysis without separation of the cathodic and anodic spaces, the working iridium-plating electrolyte acquires darker crimson color. The subsequent heat treatment of the electrolyte for 1.5–2 h leads to the restoration of the initial orange-red color of the solution.

Studying cathodic processes that occur in the course of electrochemical reduction of iridium complexes formed in sulfamate iridium-plating electrolytes is complicated by the fact that the composition and structure of these complexes are unknown. The change in the color of the working iridium-plating electrolyte relative to the initial electrolyte solution suggests the formation of new iridium complexes. These differences, along with the visual observations, are confirmed by spectrophotometric data (Fig. 2).

In the absorption spectra of the initial solution (Fig. 2, curve *1*), there are absorption bands at 229, 304, 413, 434, and 486 nm, which, according to published data [26], correspond to chloride complexes of tetravalent iridium, $[IrCl_6]^{2-}$. In aqueous solutions, the complex ions $[IrCl_6]^{2-}$ under common conditions are relatively stable, and the aquation and hydrolysis occur very slowly. The stability constant of the $[IrCl_6]^{2-}$ ion, log β, is 31 [26]. In the absorption spectra of the working iridium plating electrolyte heat-treated for 4 h, the above bands are absent, and a peak at 280–308 nm, a shoulder at 350–370 nm, and a very weak long-wave absorption band at 738 nm are observed (Fig. 2, curve *2*).

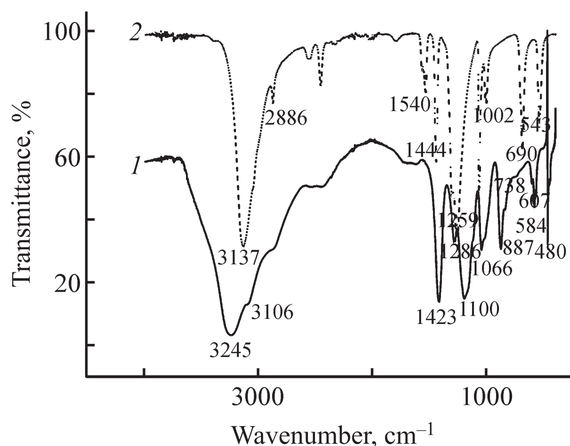

Fig. 3. IR spectra of (*1*) sulfamate iridium-plating electrolyte and (*2*) sulfamic acid. Initial electrolyte composition (g L^{-1}): $H_2[IrCl_6]$ (in terms of iridium) 5 and H_3NSO_3 50.

In [13, 27], "yellow" and "green" iridium sulfamates were prepared electrochemically in a sulfamate electrolyte. They were assumed to have the following formulas: "yellow" iridium sulfamate, $H_3[Ir_2(NH_2SO_3)_4O_3(H_2O)_2]\cdot 5H_2O$; "green" iridium sulfamate, $H_3[Ir_2(NH_2SO_3)_6O(OH)_2]\cdot 2H_2O$. Beznosyuk and Fomina [28] suggested various structural models for electrochemically active "yellow" iridium sulfamate complexes; one of them is as follows:

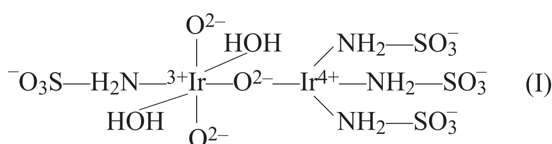

The iridium complexes under consideration can have somewhat different ligand composition. For example, they contain chloride ions instead of two other oxo ions, hydroxide ions, and other ligand from the reaction medium.

The bands in the electronic absorption spectra of the iridium-plating electrolyte were assigned taking into account published data on the electrochemical oxidation and reduction of iridium mono-μ-oxo dimers [29]. The absorption bands with the main peak at 308 nm are characteristic of hydroxo dimers of trivalent iridium, Ir(III, III), which have yellow color. The absorption spectrum of the oxo dimer of tetravalent iridium, Ir(IV, IV), has blue color and exhibits strong absorption near the red edge of the visible range with the main peak at 732 nm. Presumably, the iridium complex is a binuclear oxygen-bridged iridium complex (Ir–O–Ir) in which one Ir atom occurs in the trivalent state and the other, in the tetravalent state, Ir(III, IV).

The formation of binuclear oxygen-bridged iridium sulfamate complexes is confirmed by the IR spectra. The spectra (Fig. 3) were interpreted taking into account published data on the band assignments in the spectra of sulfamic acid [30] and related monomeric sulfamate complexes of platinum metals [31]. Comparison of the IR spectra of sulfamic acid and iridium complexes under consideration shows that the frequencies of the antisymmetric, $\delta_{as}(NH_2)$, and symmetric, $\delta_s(NH_2)$, bending bands of the NH_2 group are shifted toward lower values by 120 and 160 cm^{-1}, respectively. Such changes in the frequency can be attributed to the coordination of sulfamic acid with the iridium atom via nitrogen atom [31]. The observed shift of the frequency of the N—S stretching vibrations from 690 cm^{-1} for free sulfamic acid to 732 cm^{-1} also suggests the coordination of sulfamate ligands with the iridium atom via nitrogen atom. The higher value of ν_{as}(N—S) is due to the higher strength of the N—S bond in the iridium sulfamate complex compared to sulfamic acid [31].

In the IR spectrum of the iridium compound under consideration (Fig. 3, curve *1*), there is a relatively strong absorption band at 878 cm^{-1}. According to [32, 33], the absorption bands at 760–880 cm^{-1} are characteristic of antisymmetric stretching vibrations of binuclear oxygen-bridged complexes of platinum and other transition metals, ν_{as}(M–O–M), having linear structure. For binuclear oxygen-bridged Ru(IV) and Os(IV) complexes, the corresponding absorption bands are observed at 886 and 848 cm^{-1} [33]. The IR spectra of monomeric sulfamate complexes of platinum metals do not contain such bands [31]. The IR spectrum of "yellow" iridium sulfamate has the following absorption bands: 3037–3360, 1400–1470, 1100–1220, 857–884, and 600 cm^{-1} [27]. The appearance of the absorption band at 857–884 cm^{-1} also suggests the bridging structure of this complex. The absorption bands at 606–584 and 460 cm^{-1} can be assigned to Ir–O and Ir—OH_2 coordination bonds (iridium aqua complexes), respectively [34, 35].

Thus, our spectroscopic data in combination with published data [12, 27–34] suggest that the major species present in the working iridium-plating electrolyte are binuclear oxygen-bridged iridium sulfamate complexes in which one iridium ion is in the +3 oxidation state, and the other, in the +4 state. The current efficiency

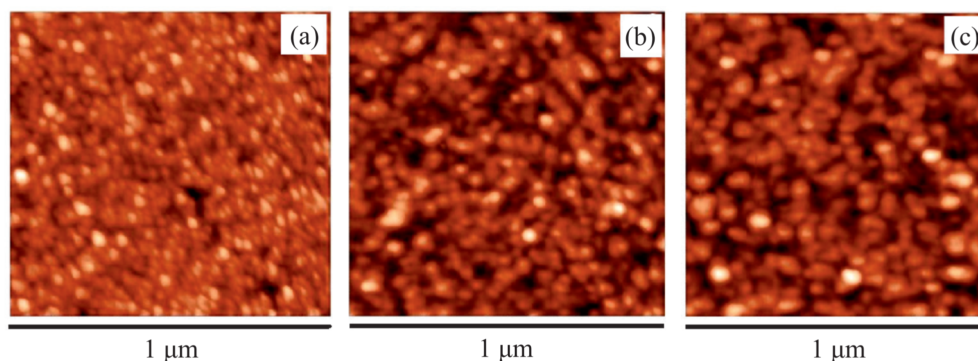

Fig. 4. Atomic-force microscopic image of the relief of the iridium film in Ir–GaAs contacts (a) 500, (b) 50, and (c) 5 μm in diameter. Initial electrolyte composition (g L^{-1}): $H_2[IrCl_6]$ (in terms of iridium) 5 and H_3NSO_3 50; current density 3 mA cm^{-2}; temperature 25°C; no stirring.

of the iridium deposition was calculated assuming the mean (overall) iridium oxidation state +3.5. Additional studies are required to determine the empirical formula and specific structure of the iridium complexes.

The surface morphology of the iridium coatings was studied for the Ir–GaAs contacts with the diameters of 500, 50, and 5 μm, obtained by electrochemical deposition without stirring (Fig. 4). The finely grained structure is clearly seen. The mean grain size somewhat increases with a decrease in the contact diameter from 25–30 nm at a contact diameter of 500 μm to 40 nm at a contact diameter of 5 μm [17]. As in the case of the sputtered contacts, the grain size in the iridium deposits, according to our data, is the smallest among the known electroplated contacts to GaAs, based on Ni, Pd, Rh, and Pt [3].

The nonuniformity of the metal layer thickness in contacts of different diameters, deposited without stirring, is manifested considerably more strongly (Fig. 5a). With a decrease in the contact diameter, the thickness of the iridium deposit considerably increases. This can account for an increase in the size of iridium grains in windows of small diameter. In addition to the dependence of the deposit thickness on the contact diameter, the deposit thickness appreciably increases from the contact center to the periphery. The change in the hydrodynamic conditions of the iridium deposition (stirring of the electrolyte with a magnetic stirrer) leads to leveling of the deposit thickness for contacts of different diameters (Fig. 5b).

The nonuniform deposition of iridium over the contact area and the dependence of the deposit thickness

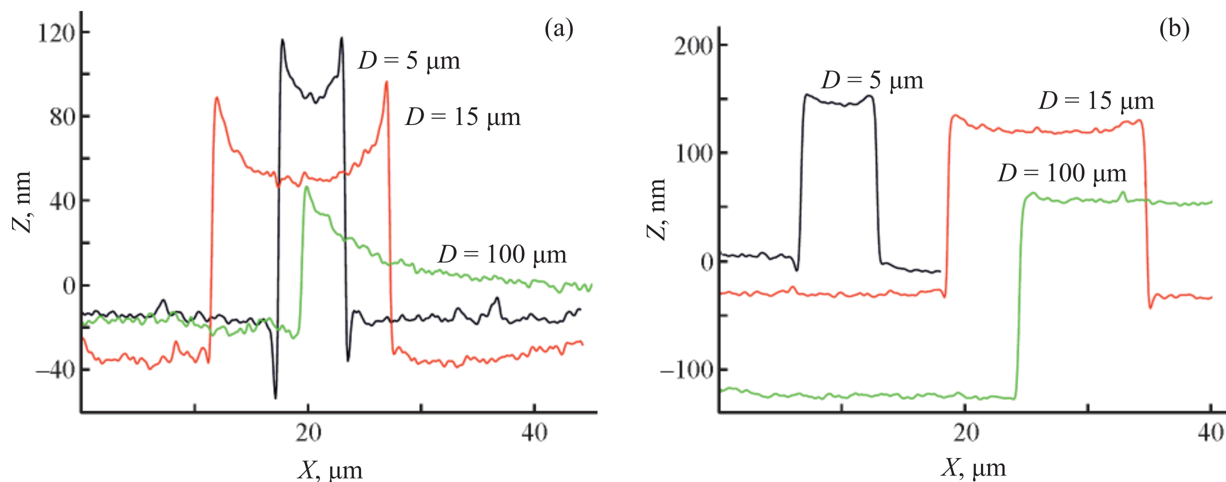

Fig. 5. Distribution of the iridium deposit thickness over the cross section of contacts of different diameters (*D*). Deposition (a) without stirring and (b) with the electrolyte stirring using a magnetic stirrer. Initial electrolyte composition (g L^{-1}): $H_2[IrCl_6]$ (in terms of iridium) 5 and H_3NSO_3 50; current density 3 mA cm^{-2}; temperature 25°C.

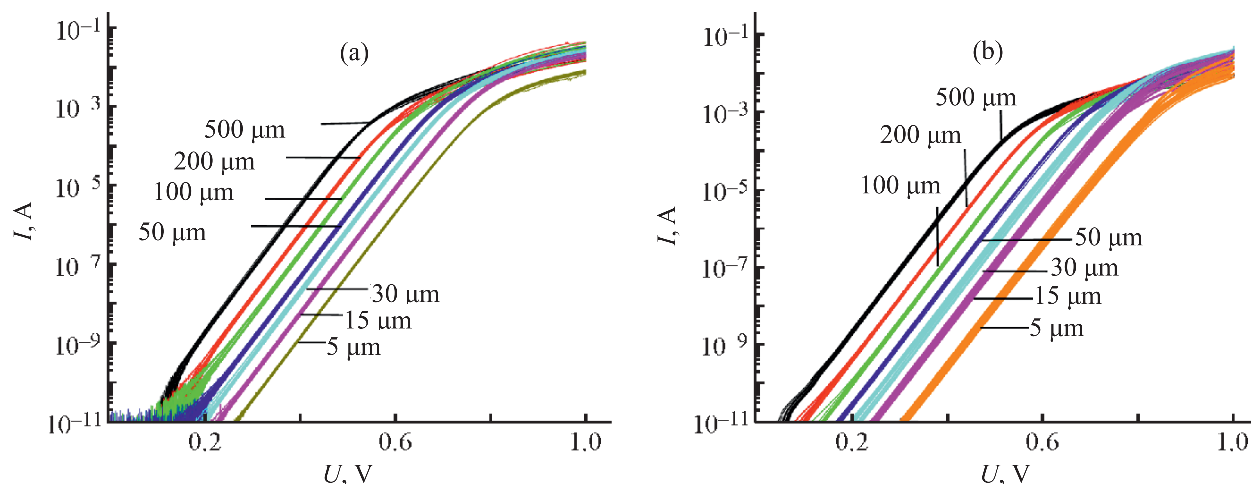

Fig. 6. Forward volt–ampere characteristics of rectifying Ir–GaAs contacts of different diameters, deposited from the iridium electrolyte (a) without stirring (20 specimens of each diameter) and (b) with stirring using a magnetic stirrer (30 specimens of each diameter). Initial electrolyte composition (g L^{-1}): $H_2[IrCl_6]$ (in terms of iridium) 5 and H_3NSO_3 50; current density 3 mA cm^{-2}; temperature 25°C.

on the window diameter are due to the so-called "edge effect" in the electrochemical deposition of the metal through the template [36, 37]. Near the template edges, the electric field lines undergo curvature (are concentrated), which leads to an increase in the local current density in this area. The iridium deposition rate at current densities corresponding to the limiting current region appreciably increases. As a result, a slight increase in the current density due to edge effects leads to a considerable increase in the deposit thickness from the contact center to the periphery. The concentration of electric field lines in windows of small diameter is higher than in windows of large diameter. Therefore, an increase in the local current density in small windows leads to an increase in the iridium deposit thickness with a decrease in the contact diameter.

The authors of [36, 37] believe that the uniformity of the thickness and the profiles of electroplated metals are mainly controlled by the current density and temperature. According to [38, 39], the edge effect can also be appreciably decreased by decreasing the width (area) of the microstructure, enhancing the electrolyte stirring intensity, or increasing the thickness of the insulating template. The kinetic relationships of the deposition can play a significant role in the process [38, 40–42]. Under the conditions of the electrochemical polarization, all the points of the cathode are equivalent, and the current density is constant over the cathode surface. In this case, the coating is deposited uniformly throughout the area of the microstructure. The diffusion (concentration) cathodic polarization makes the coating less uniform. Intense stirring of the electrolyte improves the mass transfer, decreases the diffusion layer thickness, and largely eliminates the coating nonuniformity associated with the concentration polarization [38, 41]. At current densities corresponding to the limiting current region in the cathodic polarization curve (sector *IV*), the iridium deposition occurs under mixed diffusion and kinetic control. Therefore, reduction of the diffusion limitations in stirring of the electrolyte to ensure the formation of a diffusion layer of uniform thickness largely favors the leveling of the iridium deposit thickness over the contact surface and makes it less dependent on the window diameter.

The coating deposition uniformity depends also on the geometric factors, in particular, on the anode and cathode size [36]. For electrodes of equal size, the distribution of the deposition current and deposit thickness should be uniform. Our experiments have shown that decreased ratios of the areas of the platinum electrode and semiconductor sample also ensure better uniformity of the deposit thickness in windows of different diameters and of the coating profile.

A study of the electrophysical characteristics of Ir–GaAs contacts prepared using the electrolyte that we developed confirmed their high quality [17]. Forward volt–ampere characteristics of iridium contacts (Fig. 6) obtained by electrochemical deposition without

Table 2. Mean volt–ampere characteristics (before and after annealing at 300°C) of rectifying Ir–GaAs contacts of different diameters D, deposited without stirring and with stirring using a magnetic stirrer

Contact diameter D, μm	Ideality factor n	Measured barrier height φ_{bm}, eV	Effective barrier height φ_{bi}, eV	Series resistance R_s, Ω
Without stirring				
Before annealing				
500	1.059 ± 0.0024	0.883 ± 0.0025	0.904 ± 0.0027	17.58 ± 6.371
200	1.058 ± 0.0010	0.880 ± 0.0013	0.903 ± 0.0013	16.34 ± 2.065
100	1.061 ± 0.0016	0.878 ± 0.0017	0.904 ± 0.0013	10.42 ± 3.104
50	1.072 ± 0.0023	0.871 ± 0.0061	0.901 ± 0.0012	11.73 ± 6.897
30	1.067 ± 0.0060	0.868 ± 0.0061	0.903 ± 0.0059	8.73 ± 1.076
15	1.079 ± 0.0028	0.865 ± 0.0048	0.905 ± 0.0058	8.94 ± 0.922
5	1.067 ± 0.0024	0.870 ± 0.0024	0.907 ± 0.0034	18.38 ± 2.186
Annealing at 300°C				
500	1.075± 0.0048	0.847 ± 0.0031	0.871 ± 0.0041	10.23 ± 7.791
200	1.076 ±0.0022	0.837 ± 0.0031	0.864 ± 0.0030	5.13 ± 4.060
100	1.079 ± 0.0054	0.834 ± 0.0074	0.864 ± 0.0079	9.72 ± 2.528
50	1.083 ± 0.0085	0.833 ± 0.0073	0.866 ± 0.0048	8.05 ± 1.063
30	1.091 ± 0.0043	0.825 ± 0.0030	0.865 ± 0.0019	6.57 ± 3.211
15	1.101 ± 0.0663	0.812 ± 0.0508	0.840 ± 0.0341	8.51 ± 4.336
5	1.112 ± 0.0305	0.795 ± 0.0192	0.849 ± 0.0083	16.80 ± 1.715
With stirring				
Before annealing				
500	1.057 ± 0.0047	0.886 ± 0.0032	0.906 ± 0.0602	18.45 ± 3.703
200	1.060 ± 0.0024	0.883 ± 0.0018	0.906 ± 0.0039	16.14 ± 3.947
100	1.061 ± 0.0023	0.884 ± 0.0021	0.909 ± 0.0018	14.08 ± 3.457
50	1.088 ± 0.0096	0.868 ± 0.0045	0.909 ± 0.0018	7.21 ± 1.490
30	1.084 ± 0.0056	0.874 ± 0.0037	0.913 ± 0.0048	4.83 ± 1.039
15	1.086 ± 0.0099	0.878 ± 0.0043	0.923 ± 0.0061	4.94 ± 1.731
5	1.096 ± 0.0091	0.883 ± 0.0048	0.946 ± 0.0074	9.32 ± 2.379
Annealing at 300°C				
500	1.065± 0.0017	0.846 ± 0.0054	0.866 ± 0.0030	5.96 ± 1.331
200	1.072 ± 0.0032	0.836 ± 0.0091	0.861 ± 0.0088	4.09 ± 1.016
100	1.087 ± 0.0070	0.827 ± 0.0074	0.859 ± 0.0056	3.64 ± 0.750
50	1.112 ± 0.0188	0.808 ± 0.0141	0.851 ± 0.0049	3.78 ± 0.701
30	1.159 ± 0.0119	0.804 ± 0.0064	0.852 ± 0.0028	4.60 ± 1.768
15	1.098 ± 0.0098	0.816 ± 0.0097	0.858 ± 0.0086	3.12 ± 2.114
5	1.102 ± 0.0091	0.814 ± 0.0080	0.875 ± 0.0035	7.92 ± 0.798

Table 3. Mean values of the volt–ampere characteristics (before and after annealing at 300°C) of rectifying Ir–GaAs contacts of different diameters D, deposited onto $n–n^+$-GaAs (100) structures (l = 0.3 μm, $N_D = 6 \times 10^{16}$ cm^{-3}) with stirring of the electrolyte using a magnetic stirrer

Contact diameter D, μm	Ideality factor n	Measured barrier height φ_{bm}, eV	Effective barrier height φ_{bi}, eV	Series resistance R_s, Ω
Before annealing				
500	1.048	0.900	0.919	17.682
200	1.049	0.900	0.920	15.434
100	1.052	0.898	0.921	9.644
50	1.053	0.895	0.923	9.081
30	1.058	0.893	0.930	9.442
15	1.066	0.894	0.942	3.392
5	1.084	0.889	0.946	3.812
Annealing at 300°C				
500	1.045	0.856	0.870	6.603
200	1.046	0.856	0.873	6.616
100	1.048	0.858	0.878	5.107
50	1.053	0.852	0.875	4.568
30	1.056	0.856	0.882	3.856
15	1.063	0.846	0.876	3.751
5	1.084	0.833	0.876	3.737

stirring and with stirring of the electrolyte are highly reproducible and linear on the semilog scale in a wide range of currents. The ideality factor is $n < 1.1$ for all the contact diameters, and the effective barrier height φ_{bi} is 0.90 eV and virtually coincides with the barrier height for the iridium contacts prepared by electron beam sputtering [1, 43, 44] (Table 2). Stirring of the electrolyte with a magnetic stirrer favors leveling of the iridium coating thickness throughout the window area for contacts of different diameters. A decrease in the thickness of small contacts from 200 to 90–100 nm leads to a slight increase in the ideality factor, but, on the whole, n remains lower than 1.1. The measured, φ_{bm}, and effective, φ_{bi}, barrier heights somewhat increase, and the series resistance R_s decreases (Table 2).

Low level of variance of electrophysical parameters for contacts of equal diameter also confirms high quality of Ir–GaAs contacts with the Schottky barrier. The variance of the parameters slightly increases with a decrease in the contact diameter.

The dependence of the barrier height on the metal layer thickness was noted previously [45, 46]. We have shown in this study that a decrease in the iridium deposit thickness to 35–50 nm leads to a still greater increase in the Schottky contact barrier height. For example, for the iridium coatings with the thickness of the order of 50 nm with D = 500 μm, φ_{bm} = 0.942 eV, and for D = 5 μm, φ_{bm} = 0.926 eV. For thicker contacts (90–100 nm) with D = 500 μm, φ_{bm} = 0.887 eV, and for D = 5 μm, φ_{bm} = 0.883 eV. Thus, the Schottky barrier height can be varied by varying the metal layer thickness in the contact.

We have also found that, for the semiconductor structures $n–n^+$-GaAs (100) with smaller thickness of the epitaxial layer (l) and virtually equal dopant concentration (N_D), the Ir–GaAs Schottky contacts have the volt–ampere characteristics with lower ideality factors and higher barrier height (Table 3). An increase in the effective barrier height for the semiconductor structure n-GaAs/Ti/Au/Si:AlGaAs on (100) n^+-GaAs with a thinner epitaxial layer (l =1.5 μm) is attributed in [47] to the presence of defects in the thicker layer (l = 2 μm), leading to a decrease in the barrier height and, ultimately, to worse characteristics of the diode.

The subsequent annealing of the structures obtained, performed at a moderate temperature of 300°C, leads to stabilization of the electrophysical characteristics

of the iridium contacts formed. In so doing, the ideality parameter n slightly increases for contacts of all diameters, and the series resistance R_s decreases, especially for contacts of large area. A noticeable decrease in the barrier height φ_{bm} (by 0.02–0.05 eV) upon annealing at 300°C is probably associated with a change in the structure of the intermediate oxide layer in the contact, which is accompanied by a change in its charge state, influencing the barrier height.

In this study, we also obtained high-quality iridium contacts of diameters smaller than 5 μm. For example, for the Ir–GaAs contacts with D = 3 μm, the mean ideality factor is n = 1.087 (range: 1.064–1.112; statistics: 10 specimens), and the barrier height is φ_{bm} = 0.862 eV, φ_{bi} = 0.913 eV. For the contacts with D = 1.5 μm, n = 1.095 (range: 1.079–1.112; statistics: 10 specimens), φ_{bm} = 0.862 eV, and φ_{bi} = 0.920 eV.

CONCLUSIONS

The results of determining the effective activation energy of the electrochemical reduction of iridium in a sulfamate electrolyte show that, under the optimum conditions (cathodic current density 0.3–0.5 A dm^{-2}, 20–65°C), the iridium electrodeposition occurs under kinetic control.

The iridium plating electrolyte studied mainly contains binuclear oxygen-bridged iridium(III, IV) sulfamate complexes. The iridium deposits have finely grained structure.

The iridium deposit thickness increases with a decrease in the Ir–GaAs contact diameter and in going from the contact center to its periphery. The iridium electrodeposition under the conditions of electrochemical polarization, the electrolyte stirring, and the decreased anode/cathode surface area ratios largely eliminate this effect.

A decrease in the iridium deposit thickness and in the thickness of the n-GaAs epitaxial layer leads to an increase in the barrier height of the Ir–GaAs rectifying contacts.

The iridium plating electrolyte developed allows preparation of practically ideal rectifying contacts to gallium arsenide, Ir–GaAs, including small contacts (up to 1.5 μm in diameter), with well reproducible electrophysical characteristics.

ADDITIONAL INFORMATION

Bekezina Tat'yana Petrovna, ORCID: https://orcid.org/0009-0000-9027-132X

Vaisbekker Mariya Sergeevna, ORCID: https://orcid.org/0009-0002-1078-4649

Burmistrova Viktoriya Andreevna, ORCID: https://orcid.org/0009-0000-7144-7908

Bozhkov Vladimir Grigor'evich, ORCID: https://orcid.org/0009-0008-3854-9812

ACKNOWLEDGMENTS

The spectroscopic studies and measurements by atomic-force microscopy were performed using the equipment of the Regional Center for Shared Use, National Research Tomsk State University.

CONFLICT OF INTEREST

The authors declare that they have no conflicts of interest.

REFERENCES

1. Yu, K.M., Sands, T., Jaklevic, J.M., and Haller, E.E., *J. Appl. Phys.,* 1987, vol. 62, no. 5, pp. 1815–1820. https://doi.org/10.1063/1.339562
2. Lalinsky, T., Gregušova, D., Mozolova, Z., and Breza, J., *Appl. Phys. Lett.,* 1994, vol. 64, no. 14, pp. 1818–1820. https://doi.org./10.1063/1.111988
3. Sands, T., Keramidas, V.G., Yu, K.M., Washburn, J., and Krishnan, K., *J. Appl. Phys.,* 1987, vol. 62, no. 5, pp. 2070– 2079. https://doi.org/10.1063/1.339553
4. Schulz, K.J., Musbah, O.A., and Chang, Y.A., *J. Appl. Phys.,* 1990, vol. 67, no. 11, pp. 6798–6806. https://doi.org/10.1063/1.345068
5. Jeon, C.M., Jang, H.W., and Lee, J.-L., *Appl. Phys. Lett.,* 2003, vol. 82, no. 3, pp. 391–393. https://doi.org./10.1063/1.1536246
6. Reddy, V.R., Padma, R., Reddy, M.S.P., and Choi, C.-J., *Phys. Status Solidi A,* 2012, vol. 209, no. 11, pp. 2027–2033. https://doi.org/10.1002/pssa.201228224
7. Padma, R., Lakshmi, B.P., and Reddy, M.S.P., *Superlattices Microstruct.,* 2013, vol. 56, pp. 64–76. https://doi.org./10.1016/j.spmi.2012.12.016
8. Kurmachev, V.A., *Elektronn. Tekh., Ser. 2: Poluprovodn. Prib.,* 2013, no. 1, pp. 88–89. https://www.elibrary.ru/QDFFYV
9. Ngoepe, P.N.M., Meyer, W.E., Diale, M., Auret F.D., and

van Schalkwyk, L., *Physica B,* 2014, vol. 439, pp. 119–121.

https://doi.org/10.1016/j.physb.2014.01.011

10. Grilikhes, S.Ya. and Tikhonov, K.I., *Elektrokhimicheskie i khimicheskie pokrytiya. Teoriya i praktika* (Electrochemically and Electroless-Plated Coatings. Theory and Practice), Leningrad: Khimiya, 1990.
11. Jones, T., *Met. Finish.,* 2004, vol. 102, no. 6, pp. 87–103.

    https://doi.org/10.1016/S0026-0576(04)82560-1
12. *Elektroosazhdenie blagorodnykh i redkikh metallov* (Electrodeposition of Noble and Rare Metals), Kadaner, L.I., Ed., Kiev: Tekhnika, 1974, pp. 107–114.
13. Batenkov, V.A. and Sysoeva, L.N., *Voprosy khimii. Trudy TGU. Ser. khim.* (Problems of Chemistry: Trans. Tomsk State Univ., Chemical Ser.), Tomsk: Tomsk. Gos. Univ., 1974, pp. 162–165.
14. Batenkov, V.A., Fomina, L.V., and Panov, Ya.G., *Izv. Altaisk. Gos. Univ.,* 1996, no. 1 (1), pp. 65–67. https://www.elibrary.ru/tndlfd.
15. Batenkov, V.A., Fomina, L.V., and Sarygina, E.M., in *Khimiya i khimicheskaya tekhnologiya na rubezhe tysyacheletii: Materialy II Vserossiiskoi nauchnoi konferentsii* (Chemistry and Chemical Technology at the Turn of the Millenium: Proc. II All-Russia Scientific Conf.), Tomsk, Nov. 26–28, 2002, Tomsk: Tomsk. Politekh. Univ., 2002.
16. Patent RU 2530963, Publ. 2014.
17. Bozhkov, B.G., Shmargunov, A.V., Bekezina, T.P., Torkhov, N.A., and Novikov, V.A., *J. Appl. Phys.,* 2014, vol. 115, no. 22, ID 2245505.

    https://doi.org/10.1063/1.4867778
18. Bozhkov, V.G., Bekezina, T.P., and Burmistrova, V.A., *Dokl. TUSUR,* 2022, vol. 25, no. 1, pp. 48–52.

    https://doi.org/10.21293/1818-0442-2021-25-1-48-52
19. Akchurin, R.Kh. and Marmalyuk, A.A., *MOS-gidridnaya epitaksiya v tekhnologii materialov fotoniki i elektroniki* (OMC–Hydride Epitaxy in the Technology of Materials for Photonics and Electronics), Moscow: Tekhnosfera, 2018, pp. 244–246. https://www.elibrary.ru/VLLLNY.
20. Karpovich,; N.V., Cand. Sci. Dissertation, Tomsk: Tomsk State Univ., 1990.
21. Bekezina, T.P. and Mokrousov, G.M., *Inorg. Mater.,* 2000, vol. 36, no. 9, pp. 857–863.

    https://doi.org/10.1007/BF02758691
22. Offsey, S.D., Woodall, J.M., Warren, A.C., Kirchner, P.D., Chappell, T.I., and Pettit, G.D., *Appl. Phys. Lett.,* 1986, vol. 48, no. 7, pp. 475–477.

    https://doi.org/10.1063/1.96535
23. Gorbachev, S.V., in *Trudy 4-go soveshchaniya po elektrokhimii* (Proc. 4th Meet. on Electrochemistry), Moscow: Akad. Nauk SSSR, 1959.
24. Skorobogatova, L.A., Zubritskii, S.M., Petrov, A.L., and Semenov, A.L., *Tekhnologii materialov dlya mikro- i nanoelektroniki: Uchebnoe posobie* (Technologies of Materials for Micro- and Nanoelectronics: Textbook), 2009.
25. Bozhkov, V.G., *Kontakty metall–poluprovodnik: fizika i modeli* (Metal–Semiconductor Contacts: Physics and Models), Tomsk: Tomsk. Gos. Univ., 2016.
26. Buslaeva, T.M. and Simonova, S.A., in *Analiticheskaya khimiya metallov platinovoi gruppy: Sbornik obzornykh statei* (Analytical Chemistry of Platinum Group Metals: Coll. of Review Papers), Zolotov, Yu.A., Varshal, G.M., and Ivanov, V.M., Eds., Moscow: URSS, 2003, pp. 28–29.
27. Popovich, T.N., Abstracts of Papers, *Elektrokhimicheskoe osazhdenie i primenenie pokrytii dragotsennymi i redkimi metallami: Vsesoyuznaya nauchno-tekhnicheskaya konferentsiya* (Electrochemical Deposition and Use of Precious and Rare Metal Coatings: All-Union Scientific and Technical Conf.), Kharkov, 1972.
28. Beznosyuk, S.A. and Fomina, L.V., *Izv. Altaisk. Gos. Univ., Ser. Khim.,* 2003, no. 3 (29), pp. 7–12. https://www.elibrary.ru/RDKZDL.
29. Shinha, S.B., Shopov, D.Y., Sharminghausen, L.S., Stein, C.J., Mercado, B.Q., Balcells, D., Pedersen, T.B., and Reiher, M., *J. Am. Chem. Soc.,* 2017, vol. 139, pp. 9672–9683. https://doi.org/10.1021/jacs.7b04874
30. Babu, R.R., Ramesh, R., Gopalalakrishnan, R., Ramamurthi, K., and Bhagavannarayana, G., *Spectrochim. Acta, Part A,* 2010, vol. 76, pp. 470–475. http://doi.org/10.1016/j.saa.2010.04.001
31. Griffith, W.P. and Pawson, D., *J. Chem. Soc., Dalton Trans.,* 1973, no. 5, pp. 524–526.

    https://doi.org/10.1039/DT9730000524
32. Hewkin, D.J. and Griffith, W.P., *J. Chem. Soc. A: Inorg. Phys. Theor.,* 1966, pp. 472–475.

    https://doi.org/10.1039/J19660000472
33. Griffith, W.P., *J. Chem. Soc. A: Inorg. Phys. Theor.,* 1969, pp. 211–218. https://doi.org/10.1039/J19690000211
34. Mink, J., Nemeth, Cs., Hajba, L., Sandstrom, M., and Goggin, P.L., *J. Mol. Struct.,* 2003, vols. 661–662, pp. 141–151.

    https://doi.org/10.1016/j.molstruc.2003.08.029
35. Nakamoto, K., *Infrared and Raman Spectra of Inorganic and Coordination Compounds,* New York: Wiley, 1986.
36. Li, J., Zhang, P., Wu, Y., Liu, Y.M., and Xuan, Y.M., *Microsyst. Technol.,* 2009, vol. 15, pp. 505–510.

https://doi.org/10.1007/s00542-008-0754-5

37. Luo, J.K., Chu, D.P., Flewitt, A.J., Spearing, S.M., Fleck, N.A., and Milne, W.I., *J. Electrochem. Soc.,* 2005, vol. 152, no. 1, pp. C36–C41. https://doi.org/10.1149/1.1833320
38. Hume, E.C., Deen, W.M., and Brown, R.A., *J. Electrochem. Soc.,* 1984, vol. 131, no. 6, pp. 1251–1258. https://doi.org/10.1149/1.2115796
39. Tang, J., Wang, H., Liu, R., Mao, S., Zhao, X., and Ding, G., in *2008 Int. Conf. on Electronic Packaging Technology & High Density Packaging* (ICEPT–HDP) [IEEE High Density Packaging (ICEPT–HDP), Shanghai, China, July 28–31. https://doi.org/10.1109/icept.2008.4606993
40. Asoyan, A.R., *Vestn. Saratovsk. Gos. Tekh. Univ.,* 2011, no. 2 (56), pp. 18–21. https://www.elibrary.ru/PVOOPP
41. Shul’gin, V.G., *Raspredelenie toka i povyshenie ravnomernosti osazhdeniya metallov v gal’vanotekhnike i gal’vanoplastike* (Current Distribution and Improvement of the Metal Deposition Uniformity in Electroplating), Leningrad: LDNT, 1983, pp. 6–8.
42. Medvedev, A. and Semenov, P., *Tekhnol. Electronn. Prom–sti.,* 2005, no. 4, pp. 22–24. https://www.elibrary.ru/LMXSDY
43. Barnard, W.O., Myburg, G., Auret, F.D., Goodman, S.A., and Meyer, W.E., *J. Electron. Mater.,* 1996, vol. 25, no. 11, pp. 1695–1702. https://doi.org/10.1007/s11664-996-0024-1
44. Myburg, G., Auret, F.D., Meyer, W.E., Louw, C.W., and van Staden, M.J., *Thin Solid Films,* 1998, vol. 325, nos. 1–2, pp. 181–186. https://doi.org/10.1016/s0040-6090(98)00428-3
45. Ozdemir, A.F., Goksu, T., Yildirim, N., and Turut, A., *Physica B: Phys. Cond. Matter,* 2021, vol. 616, ID 413125. https://doi.org/10.1016/J.physb.2021.413125
46. Biber, M., Güllu, O., Forment, S., Meirhaeghe, R.L. Van, and Turut, A., *Semicond. Sci. Technol.,* 2006, vol. 21, no. 1, pp. 1–5. https://doi.org/10.1088/0268-1242/21/1/001
47. Al-Ahmadi, N.A., *Heliyon,* 2020, vol. 6, no. 9, ID e04852. https://doi.org/10.1016/j.heliyon.2020.e04852

Publisher’s Note. Pleiades Publishing remains neutral with regard to jurisdictional claims in published maps and institutional affiliations.